American Mineralogist, Volume 95, pages 1399–1407, 2010

Enhancement of solid-state reaction rates by non-hydrostatic stress effects on polycrystalline diffusion kinetics

Lukas M. Keller,[1,*] Lutz C. Götze,[2] Erik Rybacki,[3] Georg Dresen,[3] and Rainer Abart[4]

[1]EMPA, Swiss Federal Laboratories for Materials Testing and Research, Überlandstrasse 129, 8600 Dübendorf, Switzerland
[2]Institute of Geological Sciences, FU Berlin, Malteserstrasse 74-100, D-12249 Berlin, Germany
[3]GeoForschungsZentrum Potsdam, D-14473 Potsdam, Germany
[4]Department of Lithospheric Research, University of Vienna, Althanstrasse 14, A-1090 Wien, Austria

Abstract

Reaction layer growth between two chemically different solids may be controlled by polycrystalline diffusion kinetics in the growing phase. The kinetics depend on the interplay between volume and grain boundary diffusion. Using spinel formation between single crystals of periclase and sapphire as an example, we quantify the effects of an applied mechanical stress on the bulk-transport properties of the reaction layer. The rate of spinel growth increases fourfold when stress normal to the reaction interface increases from 3 to 30 MPa due to stress-induced changes in grain boundary structure. At low applied stress, low-index (i.e., Σ3) "coincidence site lattice" grain boundaries with slow diffusion coefficients dominate, related to epitactic growth of spinel on sapphire. Increasing stress triggers epitactic growth of spinel on periclase, and causes sapphire-grown spinel grains to rotate out of epitaxy, and grain boundaries with fast diffusion coefficients dominate. This effect outweighs the hitherto emphasized influence of grain size on the bulk transport properties of polycrystals.

Keywords: Spinel, mineral reaction, reaction kinetics, epitaxy, non-hydrostatic stress

Introduction

The nucleation and growth of new phases in rocks, ceramics, and metals often occurs along the interface between two reacting phases (e.g., Schmalzried 1962; Joesten and Fisher 1988; Ashworth and Sheplev 1997; Carlson and Johnson 1991; Joesten 1991). Commonly, new phases form polycrystalline layers along the reaction interface leading to spatial separation of the reactant phases. Progress of the reaction may then be controlled by diffusion across the growing layer. This diffusion mass transfer may occur by a combination of volume and grain boundary diffusion (Keller et al. 2006, 2008). In many cases, the growth behavior of a reaction rim can be approximated by a kinetic law, $\Delta x^n = kt$, where Δx is the thickness of the reaction layer, k is a rate constant, t the time, and n is a parameter that accounts for the diffusion regime (Schmalzried 1962; Irving 1964; Fisher 1978). Provided that effective bulk transport properties of the reaction layer are constant with time, layer growth follows a parabolic kinetic law ($n = 2$). Then, the rate constant k (m^2/s) depends essentially on bulk diffusion of the rate limiting chemical component in the growing reaction layer. Parabolic growth was found in many previous experimental reaction rim studies (Whitney and Stubican 1971; Fisler and Mackwell 1994; Yund 1997; Watson and Price 2002). The effect of grain boundary diffusion on bulk diffusivities is commonly addressed by describing diffusion as a weighted average of the grain boundary diffusion coefficient and the lattice diffusion coefficient (e.g., Kaur et al. 1995; Harrison 1961). One fundamental assumption inherent in this approach is that all grain boundaries have similar transport properties and potential effects of grain boundary character are disregarded. Non-isostatic stress and deformation may produce texture and thus have an influence on the character of grain boundaries.

The effects of non-isostatic stress on the kinetics of diffusional phase transformations have not been investigated previously. The influence of differential stress on reaction kinetics is manifold (Wheeler 1987; Kenkmann and Dresen 1998; Stünitz and Tullis 2001; Heidelbach et al. 2009). In particular, plastic deformation may influence grain boundary density due to the formation of subgrains (Poirier 1985; Hay 1994). However, since the diffusivities along a specific grain boundary depend also on the boundary structure (Sutton and Baluffi 1995; Kaur et al. 1995), the chemical transport rates in stressed reaction layers may depend not only on the grain boundary density, but also on the distribution of grain boundary types with different structures. Furthermore, deformation of starting material and reaction products may increase dislocation density providing fast diffusion pathways along dislocation cores. So far, the effect of stress- and strain-induced changes of the defect structure on bulk transport properties have not been investigated in the context of reaction layer growth. The magnitude of non-isostatic stress needed to modify individual microstructural parameters in reaction layer growth is unknown. In addition, the microstructure of a polycrystal that forms between two reacting phases may be imprinted by epitactic growth on the reactant phases, but it is largely unknown how such a microstructure is modified by deformation under differential stress.

* E-mail: Lukas.Keller@empa.ch

0003-004X/10/0010–1399$05.00/DOI: 10.2138/am.2010.3372

To reveal the stress effects on microstructural properties and their coupling to the transport properties of a polycrystal, we experimentally investigated the reaction of periclase (MgO) + sapphire/corundum (Al_2O_3) → spinel ($MgAl_2O_4$). Periclase single crystals and both sapphire single crystals and corundum polycrystals were used as starting materials. Polished MgO and Al_2O_3 cubes of 3 × 3 × 5 mm edge length were carefully aligned and loaded in a creep apparatus (Freund et al. 2004) and annealed at 1350 °C and ambient pressures for 157 h. Three runs were performed at uniaxial stresses of 2.9, 14.5, and 29.0 MPa oriented normal to the interface between the reacting crystals. Dry conditions were maintained by applying a flow of dry argon in the furnace chamber. The microstructure evolution and dislocation densities of the spinel reaction layers were investigated using electron backscatter diffraction (EBSD) and transmission electron microscopy (TEM). Inferences are drawn with respect to the influence of microstructure and texture on the bulk transport properties of the spinal polycrystal and epitactic relations at reaction interfaces are discussed in the context of texture formation.

Experimental methods

Experiments

The experiments were conducted in a dead load creep apparatus at T = 1350 °C with a run duration of 157 h. Experiments at differential stresses (i.e., $\sigma_d = \sigma_1$) of 2.9, 14.5, and 29 MPa were performed by varying the applied dead-weight on the top of the assembly (Fig. 1). Starting materials in the form of cubes were cut and the reaction faces (3 × 3 mm) were ground and polished. Then, cube piles with the stacking sequence polycrystalline-corundum/MgO-boule/sapphire-boule were assembled and placed between two alumina pistons. This configuration was chosen to unravel the effects of polycrystalline vs. single-crystal nature of reactants on the kinetics of spinel formation. The crystallographic orientations of MgO and sapphire boules with respect to the reaction interface are given along with the results (Fig. 2). Experiments were performed under constant argon flow. Further details concerning temperature, stress, and strain monitoring as well as other technical details can be found in (Götze et al. 2009), who conducted similar experiments on spinel-forming reactions using the same experimental procedure.

Crystal orientation imaging

The internal microstructure of a spinel reaction rim was investigated by electron backscatter diffraction and forward scatter electron (FSE) imaging using a TSL DigiView EBSD detector system attached to a Quanta 3D FEG FIB-SEM (Scanning Electron Microscope) instrument. The specimen surface was chemo-mechanically ultra-polished by using a colloidal silica suspension for EBSD analysis without carbon coating. Charging of the sample surface was mitigated by setting the chamber pressure to 30 Pa. Automated beam scans were performed on a square raster with a step size of 0.25–0.50 µm over a selected area. The TSL software OIM 5.2 was used to collect, index, and analyze the EBSD patterns. The data sets were filtered to remove non-reliably indexed measurements (filter criterion: confidence index >0.1). Orientation maps and pole figures represent crystal and lattice planes orientations with respect to a horizontal (east-west) reaction interface.

Note, that a full macroscopic characterization of a grain boundary requires the knowledge of the orientation of the grain boundary plane and the orientation relation between the lattices of the two adjacent grains. Five parameters are needed to describe these orientation relations: three defining the rotation axis and rotation angle (i.e., the misorientation ω) that relates the two crystal lattices and two defining the normal to the grain boundary plane, which describes the orientation of the grain boundary plane. Using EBSD mapping, it is possible to measure only four out of the five parameters from a single section plane. The fifth parameter, the inclination of the boundary with respect to the section plane, can be determined either by serial sectioning (Saylor et al. 2003) or stereological considerations (Saylor and Rohrer 2002).

EBSD provides the full crystallographic orientation (i.e., in OIM defined as the rotation to bring the sample reference frame into coincidence with the crystal reference frame) of each point (see Figs. 2a, 2c, and 2e). Crystal orientation imaging can map and/or characterize grain boundaries in many different ways. Most fundamental is the misorientation angle (i.e., the smallest angle of rotation leading from one orientation into another). OIM may be used to map boundaries where the misorientation between two neighboring grains falls within a user-defined range of rotation angle. Then fractions and densities of grain boundaries specific misorientation angles can be calculated from the boundary length and area (see Figs. 4b–4c). In addition, OIM can identify and map "coincident site lattice" (CSL) boundaries of cubic materials between two neighboring grains. In the CSL concept, the lattices of two neighboring crystals are expanded until they interpenetrate. It is found that several lattice sites coincide forming a sublattice pertaining to both crystals, which is referred to as the CSL. The degree of coincidence is quantified by Σ = 1/n, where n is the fraction of lattice sites that are common in both crystals. Thus, a grain boundary that contains a high density of lattice points in the CSL (i.e., low Σ values) has good atomic fit (Balluffi et al. 1982). If the misorientations of neighboring grains are within a given tolerance of specified CSL then the respective grain boundary is classified with respect to its Σ and highlighted with a specific color code on the crystal orientation map (in Fig. 2, Σ3 grain boundaries are indicated by yellow lines). The tolerance in misorientation angle for assigning a specific Σ is given by $\Delta = K/\Sigma^n$, the so-called Brandon's criterion. K and n were set to the common values of 15° and 0.5, respectively. Regarding the meaning and significance of Brandon's criterion, the interested reader is referred to the review of King and Shekhar (2006) and references therein. The fraction of Σ3 boundaries, which in the axis/angle description corresponds to a rotation of 60° around [111], is shown in Figure 4d. In Figure 4d, the fraction of Σ3 boundaries is compared to the fractions of low-angle (ω < 5°) and high-angle (ω > 5°) grain boundaries.

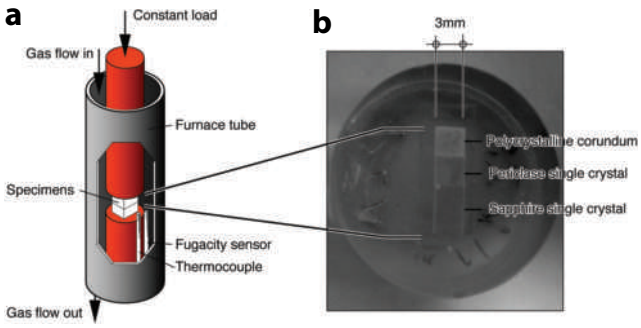

Figure 1. (**a**) Schematic drawing of the uniaxial creep apparatus (modified after Freund et al. 2004). (**b**) Photo of the assembly configuration (see text for further explanations).

Transmission electron microcopy

Dislocation densities were investigated by preparing site-specific TEM foils with the dimension 15 × 10 × 0.150 µm using the focused ion beam (FIB) technique (Quanta 3D FEG). TEM investigations were done on a Tecnai F20 X-Twin transmission electron microscope operated at 200 kV with a field emission gun (FEG) as electron source.

Microstructure evolution

The internal microstructure of the spinel reaction layers formed from periclase and sapphire single crystals is shown in Figure 2. On the LHS crystal, orientation maps of the spinel layers are shown. The white areas below and above the color-coded maps correspond to periclase and sapphire single crystals, respectively. The color-coding indicates distinct orientations of the spinel grains and/or specific orientation relations to the reactant phases (see captions for more information). On the RHS, the colors in the pole figures of sapphire correspond to the colors of the maps, and the pole figures show the orientations of selected crystallographic planes. In the pole figures, the reaction interface is horizontal. The microstructure of the spinel layers that formed from polycrystalline corundum and single crystals

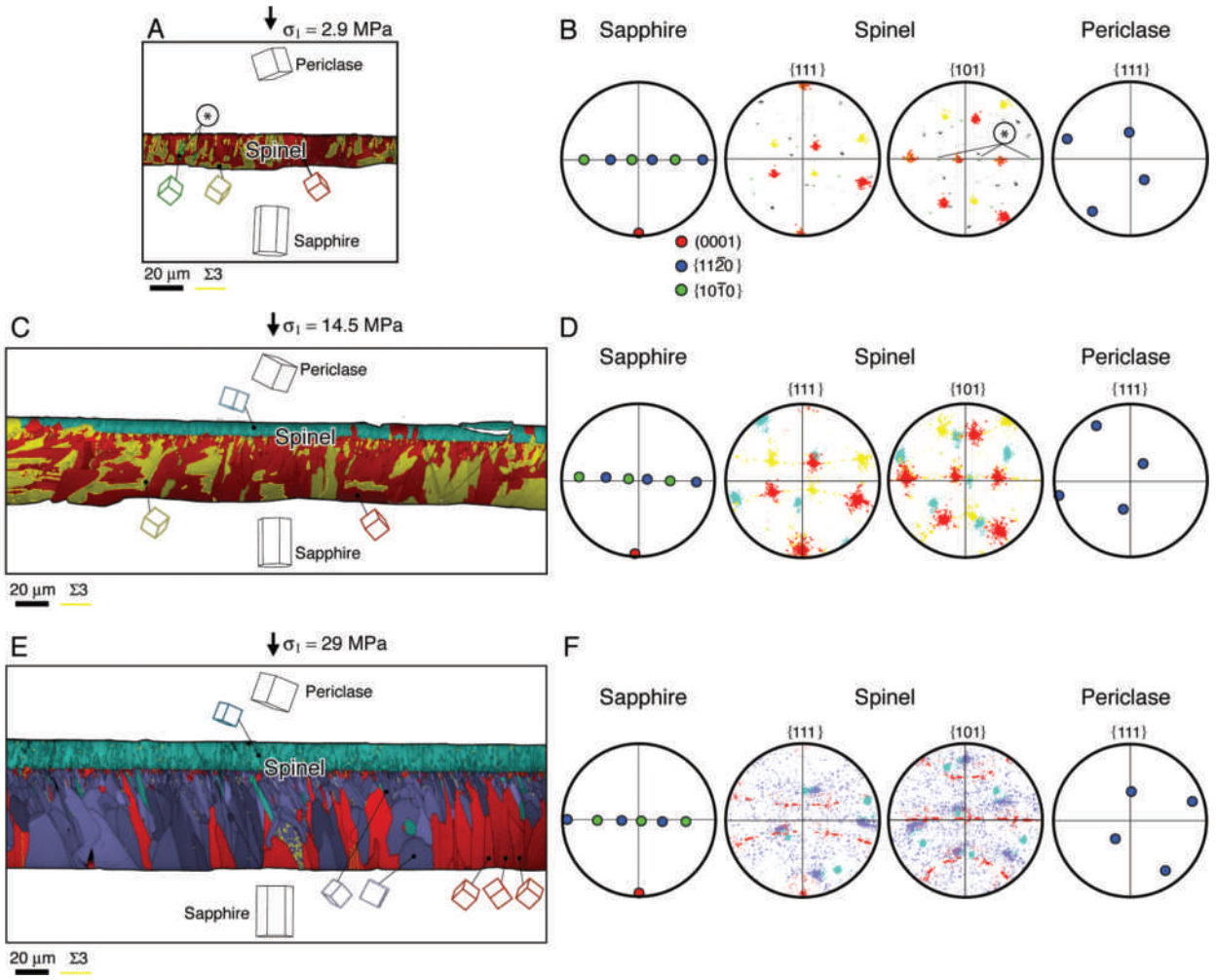

FIGURE 2. Microstructure of spinel reaction layers formed at the interfaces of periclase and sapphire single crystals. (**a**, **c**, and **e**) Crystal orientation maps of reaction layers produced at vertical stresses of 2.9, 14.5, and 29 MPa, respectively. All experiments were done at 1350 °C and for similar run durations of 157 h. The reaction interfaces are horizontal, the upper interface corresponds to the spinel-periclase boundary, and the lower interface corresponds to the spinel-sapphire boundary. The background gray levels reflect the EBSD pattern quality parameter (IQ) outlining the grain boundaries. Overlay colors mark grains with distinct orientations and/or orientation relations to the reactant phases. In **a**, the red and yellow grains have the same epitaxial relations to sapphire, where the two orientations are related through a 60° rotation about $[111]_{Spinel}$. The green grains marked by an encircled asterisk have an additional epitaxial relation to sapphire (see text). In **c** and **e**, the spinel layer at higher stresses is comprised of two microstructurally distinct layers. The turquoise layers show epitaxy after periclase (note unit cells). In **c**, the layer with red and yellow grains shows epitaxy to sapphire with similar color-coding as above. In **e**, the thick layer with red and gray-blue grains is sapphire-grown spinel. Red grains show $[111]_{Spinel}||[0001]_{Sapphire}$ axiotaxy (note unit cells) with sapphire and gray-blue grains have either a weak epitaxial relation to periclase or no orientation relation to the reactant phases. Unit cells show the orientation of periclase, sapphire, and of selected spinel grains. Yellow lines mark Σ3 grain boundaries. (**b**, **d**, **f**) (0001), {11$\bar{2}$0}, and {10$\bar{1}$0} pole figures of sapphire and {111} and {101} pole figures of spinel and periclase. The reaction interface is horizontal in the pole figures. The colors in the pole figures of spinel correspond to overlay colors of the maps and show the orientation of individual grains. In **b**, the encircled asterisks mark the orientation of the green grains.

of sapphire is shown by the crystal orientation map depicted in Figure 3. Both single-crystal and polycrystalline reactants produce polycrystalline spinel reaction layers (Figs. 2–3). For single-crystal reactants, we observed a strong rate dependence of spinel formation on the applied normal stress. This effect was not found in experiments performed with polycrystalline corundum as a starting material. If single crystals are used as reactant phases, layer growth increases roughly fourfold, with applied stresses increasing from 2.9 to 29 MPa (Figs. 2–4).

At 2.9 MPa, the spinel polycrystal contains a large fraction (~50%) of Σ3 CSL boundaries in addition to boundaries with misorientations $\omega < 15°$ (Figs. 2a, 2b, and 4). Toward higher stresses, the sapphire- and periclase-grown layers of the spinel rim evolve with different microstructures. Periclase-grown spinel is essentially a single grain containing numerous small-angle grain boundaries with misorienation angles $\omega = 2–5°$ and with traces nearly perpendicular to the spinel-periclase interface (Figs. 2c and 2e). In contrast, sapphire-grown spinel is polycrystalline

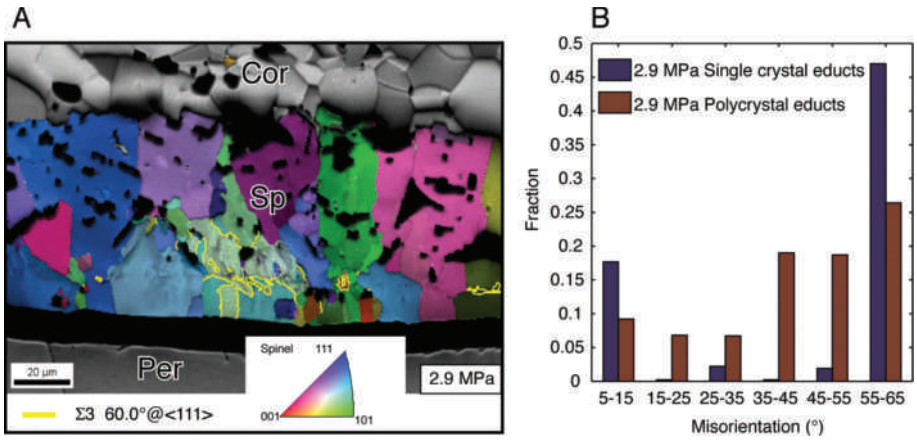

◀**FIGURE 3.** Microstructure of spinel that grew between polycrystalline corundum and a periclase single crystal at a vertical stress of 2.9 MPa. (**a**) Crystal orientation map of spinel, color key corresponds to inverse pole figure representation with respect to a horizontal direction. Background gray levels reflect the EBSD pattern quality parameter (IQ) outlining grain boundaries. Yellow lines mark Σ3 grain boundaries. (**b**) Fractions of grain boundary misorientation angles of 10° bins up to 65°. Blue bars = spinel between single-crystal reactant phases at 2.9 MPa, brown bars = spinel between polycrystalline reactant phases at 2.9 MPa.

and the average grain size increases from 1.3 µm at 2.9 MPa and 2.8 µm at 14.5 MPa to 4.3 µm at 29 MPa. Spinel typically displays straight grain boundaries separating grains with high aspect ratio. The observed enhancement of the reaction rate with increasing stress is thus completely unexpected considering the concomitant increase in grain size. This apparent dichotomy can be understood by considering the stress-induced change in the distribution of grain boundaries with different misorientation. In particular, grain boundary misorientations are successively more widely distributed toward higher stresses (Fig. 4), and the densities of grain boundaries with misorientations between 15 and 55° are highest at the largest imposed stresses (Fig. 4). In contrast, at low stress most grain boundaries show misorientations $\omega < 15°$ and $\omega > 55°$. Note that the density of Σ3 boundaries continuously decreases with increasing stress. Based on the assumption that grain boundary diffusion contributed appreciably to bulk material transfer across the polycrystalline spinel rim, this suggests that the stress-induced growth rate amplification is caused by a change in the grain boundary character distribution and the associated enhancement of bulk diffusivities (Figs. 2 and 4).

Single-crystal vs. polycrystalline reactants

If corundum polycrystals are used as starting materials together with periclase single crystals, there is no profound effect of differential stress on the rate of spinel formation between polycrystalline oxides (Götze et al. 2009). At similar conditions, they observed a spinel rim thickness similar to the rim thickness that in our study was grown between single-crystal oxides at the highest imposed stresses (Fig. 4a). For polycrystalline reactants, the rim of newly formed spinel is composed of numerous elongated grains, which form a palisade-like microstructure perpendicular to the reaction interfaces (Fig. 3a). The spinel grains show random crystallographic orientations without any systematic orientation relation to either corundum or periclase (Götze et al. 2009). The spinel grains are mostly separated by grain boundaries with large misorientation angles $\omega > 15°$ (Fig. 3b) and in this respect inherit the characteristics of the reactant corundum polycrystal. This suggests that the grain boundary character distribution in the spinel rim is largely controlled by the nature of the reactant corundum. The inheritance of a microstructure with a high density of grain boundaries with large

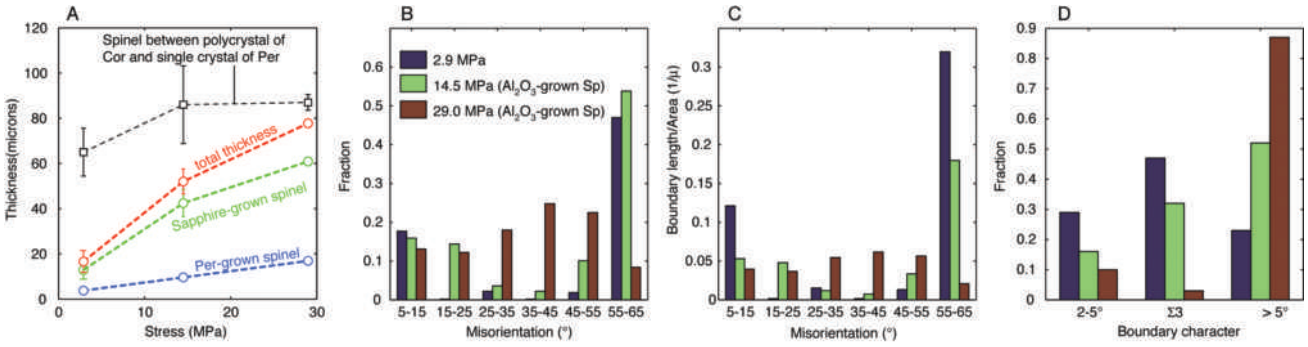

FIGURE 4. We compare the thickness of spinel reaction layers and distributions of fractions of grain boundary misorientation angles, misorientation densities, and fractions of CSL boundaries. (**a**) Dependence of layer thickness an applied stress. Blue = spinel grown into periclase, green = spinel grown into sapphire, red = total layer thickness; dashed lines and open circles correspond to spinel growth between single-crystal educts. Black dashed lines and open squares correspond to spinel growth between polycrystalline corundum and a single crystal of periclase. The error assigned to the symbols is two sigma on repeated measurements. (**b**) Fractions of misorientation angles of 10° bins up to 65°. (**c**) Misorientation densities of 10° bins up to 65°. (**d**) Fractions of small angle grain boundaries (ω = 2–5°), Σ3 boundaries, and grain boundaries with $\omega > 5°$. Blue bars = sapphire-grown spinel at 2.9 MPa, green bars = sapphire-grown spinel at 14.5 MPa, and brown bars = sapphire-grown spinel at 29 MPa.

misorientation angles enhances diffusion and leads to rapid reaction rim growth, irrespective of the applied vertical stress.

Applied stress and defect density

Transmission electron microscopy (TEM) reveals a significant increase of dislocation densities in spinel with increasing applied stresses. In spinel from samples annealed at 2.9 MPa, dislocations are largely absent, but the dislocation density increases up to 1e + 13 m^{-2} in samples annealed at stresses of 29 MPa (Fig. 5). The same dependence of defect density on applied stress is observed in both experiments with single-crystal sapphire and with polycrystalline corundum as a starting material. Stress-induced defects hence cannot explain the stress-enhanced growth rate, which is only observed, if sapphire single crystals are used.

Epitactic relations

At stresses of 2.9 MPa spinel overgrowths formed from both sapphire and periclase show the same strong and well-known epitactic relations with respect to sapphire (Rossi and Fulrath 1962). Interestingly, the spinel grains show only three crystal-

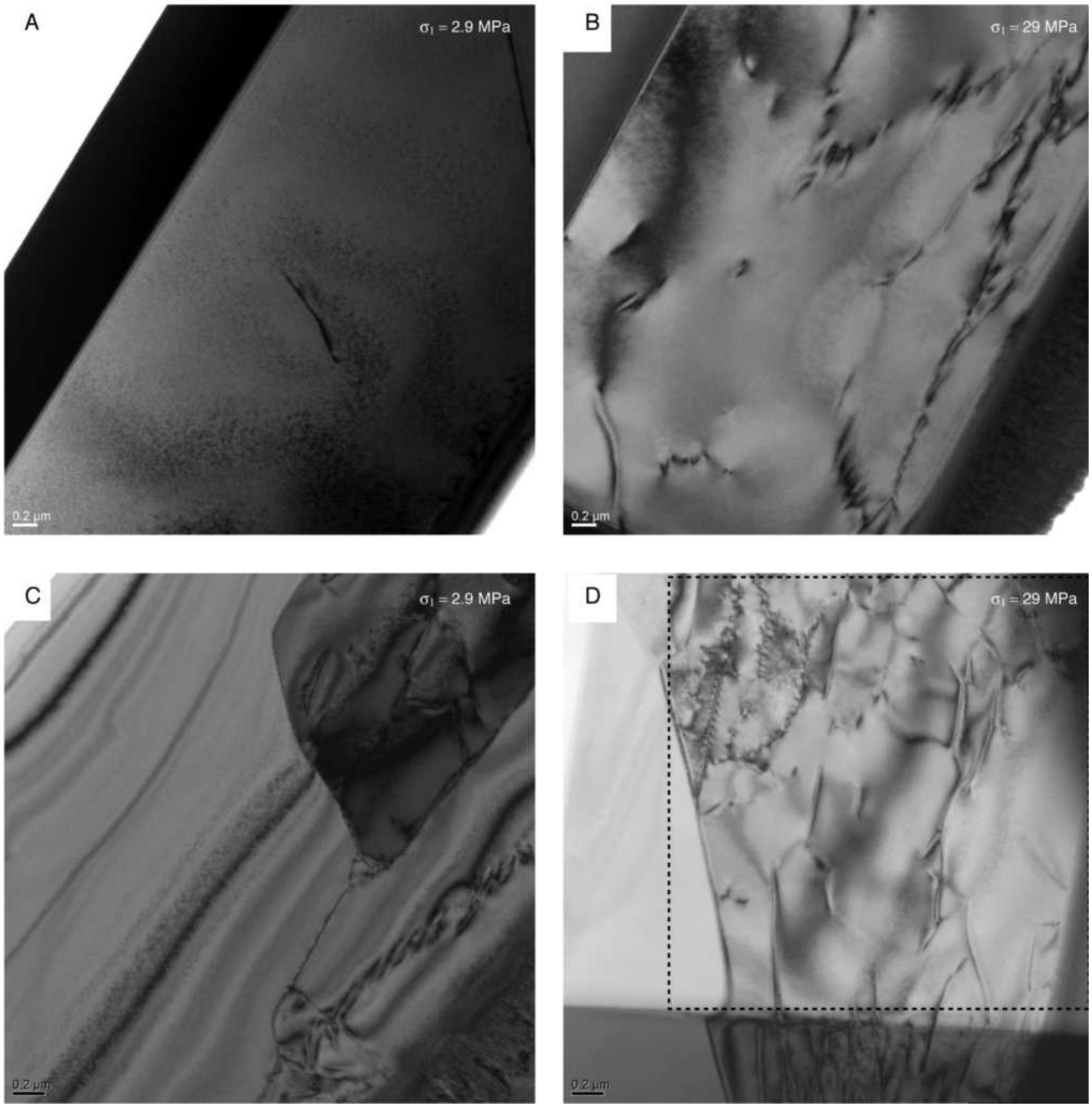

Figure 5. Bright-field transmission electron images showing dislocation microstructures in spinel. (**a** and **b**) Spinel formed between polycrystalline corundum and single crystals of periclase at a vertical stress 2.9 MPa (**a**) and 29 MPa (**b**). (**c** and **d**) Spinel formed between single crystals of sapphire and single crystals of periclase at a vertical stress 2.9 MPa (**c**) and 29 MPa (**d**). The dislocation density used in the text was determined for the volume marked by the dashed rectangle.

lographic orientations, two of which predominate and are related to multiple twinning (i.e., 60° at [111]). Because the [111] twin axis is parallel to [0001] of sapphire the crystal twins show the same orientation relations to sapphire, $[111]_{Spinel}||[0001]_{Sapphire}$ and $(110)_{Spinel}||(10\bar{1}0)_{Sapphire}$ (red and yellow grains in Figs. 2a–2c) and are separated by Σ3 twin boundaries. The third orientation is occupied only by a few grains (green grains in Figs. 2a–2b) and shows the relation $[111]_{Spinel}||[0001]_{Sapphire}$ and $(110)_{Spinel}||(11\bar{2}0)_{Sapphire}$. These grains are separated in part by near Σ13 grain boundaries (i.e., 27.8° at [111]). The common [111] rotation axis for both misorientations is perpendicular to the reaction interface and is parallel to [0001] of sapphire. Note that spinel formed from periclase is epitactic with respect to sapphire in the 2.9 MPa experiment. This was also observed by earlier workers (Rossi and Fulrath 1962), who produced spinel reaction rims between periclase and corundum single crystals at near atmospheric pressures.

In contrast, higher normal interface stresses trigger the formation of two epitactic spinel layers, which grow oriented with respect to sapphire and periclase, respectively (Figs. 2c–2f). This also indicates that the structural boundary between these layers marks the position of the original sapphire-periclase interface. At the highest imposed stress of 29 MPa, the epitaxial relation between sapphire and spinel weakens. The relation between (110) of spinel and the $(10\bar{1}0)$ of sapphire is successively lost and only the axiotaxy with $[111]_{Spinel}||[0001]_{Sapphire}$ is retained (Figs. 2e–2f). In addition, some of the sapphire-grown spinel grains show a weak epitaxy after periclase (some of the gray-blue grains in Figs. 2e–2f) and several grains do not show any epitaxial relation with the substrate at all.

DISCUSSION

Interface crystallography and diffusion mechanism

The growth kinetics of solid-state transformations are controlled by a combination of two types of processes. The kinetics involves structural and chemical changes at moving reaction interfaces as well as diffusion of matter across the growing reaction layer. If the diffusion process is rate limiting, the kinetics is referred to as diffusion controlled and the rim thickness increases proportional to the square root of time. Spinel growth may occur through a variety of diffusion mechanisms (e.g., Schmalzried 1981). Maintenance of charge neutrality requires that the fluxes of diffusing species couple. Thereby, three limiting diffusion couples are possible: (1) Mg^{2+} and O^{2-}; (2) 2 Al^{3+} and 3O^{2-}; and (3) 3 Mg^{2+} and 2 Al^{3+}. The latter is called counter diffusion of cations (Mg^{2+}, Al^{3+}) (Koch and Wagner 1936). Note that the position of the original sapphire-periclase interface depends on the half reactions that proceed at the reaction interfaces, which in turn depend on the diffusing species (see below). Combinations 1 and 2 involve diffusion of relatively large oxygen anions, which is a less likely scenario since the phases and interfaces involved are dense and thus, do not provide diffusion channels for large anions (Hesse et al. 1994). Combination 3 requires the HCP anion lattice of sapphire to be modified into the FCC lattice of spinel. Concerning this modification, the "extent" of reconstruction depends on the orientation relationships along the initial sapphire-periclase or the sapphire-spinel interface. Previous studies often focused on the sapphire(0001)/periclase(111) and sapphire(0001)/spinel(111) interface relations (e.g., Carter and Schmalzried 1985), for which the close-packed oxygen planes are parallel and the oxygen lattice transformation at the reaction interfaces occurs under semicoherent conditions (i.e., a phase boundary characterized by partial lattice matching and in which dislocations compensate for part of the lattice mismatch). These are favorable orientation relationships and the reaction interfaces are expected to move through a more or less stationary oxygen lattice. For such a case, it is reasonable to assume that spinel growth occurs by counter diffusion of cations. Regarding our experiments, the crystallographic relation between periclase and sapphire along the initial reaction interface was close to (311)/(0001) which, in terms of the low-index planes, is an incoherent interface. At low stresses, spinel grows epitactic after sapphire with the relations (111)/(0001) and (110)/$(10\bar{1}0)$. These crystallographic relations ensure a hexagonal symmetry of the close packed oxygen lattice planes in spinel and sapphire parallel to the reaction interface and the formation of a semicoherent oxygen sublattice along sapphire-spinel interface. On the other reaction interface there is the formation of a periclase(311)/spinel(111) reaction interface. This is an incoherent interface that does not permit simple reconstruction of the periclase oxygen lattice into the oxygen lattice of spinel. At intermediate stresses a sapphire(0001)/spinel(111) and a spinel(311)/periclase(311) interface develop. With respect to the oxygen sublattice these reaction interfaces are semicoherent, respectively, coherent and their formation is related to simultaneous epitactic growth of both sapphire- and periclase-grown spinel. Thus, compressive stress apparently triggers the formation of a coherent spinel/periclase reaction interface. Thereby, incoherency along the original sapphire/periclase interface is no longer accommodated at the moving spinel/periclase reaction interface but along the stationary position of the original reaction interface. In addition, semicoherency or coherency along both reaction interfaces suggest a stationary oxygen sublattice in the reactants and thus, counter diffusion of cations as reaction mechanism for spinel growth.

The reaction mechanism can also be verified by comparing a theoretical position with the observed position of the original periclase-sapphire interface within the spinel reaction rim. The half-reactions at the reaction interfaces are inferred using the compilation of the subsolidus phase relations of Hallstedt (1992) and assuming equilibrium between substrate and reaction products. A spinel composition of $Mg_{45/52.5}Al_{110/52.5}O_4$ is in equilibrium with Al_2O_3 at 1350 °C suggesting the reaction at the spinel-sapphire interface $14/3Al_2O_3 + 3Mg^{2+} - 2Al^{3+} = 3.5(Mg_{45/52.2}Al_{110/52.5}O_4)$. At the spinel-periclase interface a spinel with almost stoichiometric composition (i.e., $Mg_2Al_3O_4$) coexists with MgO that may be formed by the reaction $4MgO - 3Mg^{2+} + 2Al^{3+} = MgAl_2O_4$. From these interface reactions, the theoretical ratio of thicknesses between layers of periclase- and sapphire-grown spinel is 1/3.5. This is in excellent agreement with the thickness ratio of half-layers experimentally grown from periclase and spinel. The measured ratios of layer thickness at stresses of 2.9 and 29 MPa are 1/3.43 (±0.24) and 1/3.60 (±0.05). At 14.5 MPa, the measured ratio is 1/4.43 (±0.4). The good agreement between calculated and observed thickness ratios suggests that ionic transport across the reaction layers indeed occurred by counter diffusion of Mg and Al cations along grain boundaries.

The effect of grain boundary character distribution on bulk diffusion

We suggest that the stress-induced increase in grain boundary misorientation leads to the observed increase in the reaction rate. Regarding our experiments, the observed crystallographic relations along the reaction interfaces and the observed position of the original reaction interface suggest counter diffusion of cations as a diffusion mechanism for spinel growth (see above) given that spinel growth occurs by counter diffusion of Mg^{2+} and Al^{3+} cations. The reaction rate may be given by $\Delta x^2 = 2k\upsilon t$, where x is thickness of reaction layer, k is the reaction rate constant, and υ is the volume of spinel formed per equivalent of Mg^{2+}. The reaction rate constant is $k = zcD4/(3RT)\Delta G$, where z is absolute charge, c is the average concentration in equivalents of Mg^{2+} in the spinel layer, D is the diffusion coefficient, and ΔG is the free energy of formation of spinel from the oxides (Schmalzried 1962). To illustrate the effect of grain boundary diffusion on growth rates, we first calculate theoretical reaction rate and assume that chemical transport occurs by volume diffusion only. Published data show a large spread for values estimated for volume diffusion coefficients in spinel at the conditions of our experiments. In particular, there is discrepancy between Mg^{2+} tracer diffusion coefficients estimated on single crystals (=3e–15 m^2/s at 1350 °C) (Sheng et al. 1992) and $Mg^{2+} \leftrightarrow Al^{3+}$ interdiffusion data estimated from rim growth experiments (=1e–14 – 7e–14 m^2/s at 1350 °C) (Zhang et al. 1996; Watson et al. 2002). This discrepancy is possibly due to the contribution of grain boundary diffusion to the overall material transfer across the growing polycrystalline reactions layer. However, using the above interdiffusion coefficients, we obtain a theoretical layer thickness of 87 and 230 μm at the conditions of our experiments. These growth rates are significantly higher than the experimentally obtained rates of 16 and 52 μm at 2.9 and 14.5 MPa between single-crystal reactants (Fig. 4). This suggests that layer growth is controlled by grain boundary diffusion and that pure lattice interdiffusion in spinel is possibly even slower than Mg^{2+} tracer diffusion (<3e–15 m^2/s), which yields theoretical layer thickness of around 50 μm.

Using the above formulation of the reaction rate to calculate an effective diffusion coefficient D_{eff}, we obtain 4e–16 to 4e–15 and 8e–15 m^2/s at respective normal interface stresses of 2.9, 14.5, and 29 MPa. Thus, variation of the normal stress on the reaction interface from 2.9 to 29 MPa increases bulk diffusion in spinel by one to two orders of magnitude irrespective of a concomitant increase in average grain size. Consequently, we suggest that enhanced diffusion rates and reaction kinetics observed in experiments performed at elevated stresses are due to the stress-induced modification of the grain boundary character distribution. This offers a way to approximate the dependence of grain boundary diffusion on misorientation angle by using known values of D_{eff} and known area fractions f with specific misorientation relations. To obtain area fractions from grain boundary densities we assumed a grain boundary thickness of 1 nm. Values of D_{gb} can the be extracted on the base of Hart's equation $D_{eff} = (1 - f)D_{vol} + fD_{gb}$. For example, at low stress, the spinel layer contains solely Σ3 boundaries and low-angle grain boundaries with misorienations angles $\omega < 15°$. The Σ3 boundaries represent closely packed structures for which diffusion rates are assumed to be low (Sutton and Baluffi 1995). By assuming $D_{vol} \approx D_{gb}(\Sigma 3) << D_{gb}$ we estimate that $D_{gb}(\omega < 15°) = 2e{-}12$ m^2/s. Using this value for the experiments performed at higher stresses, we obtain values for $D_{gb}(15° < \omega > 55°)$ of 3e–11 and 4e–11 m^2/s at 14.5 and 29 MPa, respectively. These calculations suggest that grain boundary diffusion in spinel varies by one order of magnitude as the misorientation changes from 0 to 60°, which agrees well with theory (Sutton and Baluffi 1995).

Application of the above parabolic growth law and the Hart's equation to estimate values of the D_{eff} and D_{gb} assumes that bulk transport properties in the reaction layer are constant with time and that no material leaks from the grain boundary plane into the grain interiors. Leaking of material from the grain boundaries is unlikely because a driving force for diffusion out of grain boundary is largely absent in cases where the growing layer is saturated in the diffusion components (see Joesten 1991 for further discussion).

Interaction between reaction and deformation

Uniaxial loading of the reactants results in elastic and plastic deformation of substrate and reaction products. The associated elastic E_{el} and plastic strain energies E_{pl} stored in crystals reduce the driving force for the reaction. The elastic strain energy induced by uniaxial stress may be expressed as $E_{el} \approx V_m/2E\sigma_1^2$. The plastic strain energy stored by dislocations is $E_{pl} \approx V_m 0.5\rho G b^2$ (Humphreys and Hatherly 1995). The reaction ΔG with a strain energy term accounting for uniaxial stress (assuming elastic isotropy) is given by: $\Delta G_{tot} = \Delta G_{chem} + V_m/2E\sigma_1^2 + V_m 0.5\rho G b^2$, where V_m is molar volume, E is the elastic bulk modulus, ρ is the dislocation density, G the shear modulus, and b the length of the Burger's vector. Inserting the applied compressive stresses and observed dislocation densities clearly shows that the contribution of the strain energy to the total Gibbs free energy of the reaction is negligible (i.e., $E_{el} \approx 1e{-}5\Delta G_{chem}$ and $E_{pl} \approx 1e{-}3\Delta G_{chem}$ at 29 MPa). It is conceivable that the elevated dislocation densities in samples subjected to higher stresses enhance diffusion transport through the crystal lattice by pipe diffusion. However, spinel formed between polycrystalline corundum and periclase single crystals at low stresses (2.9 MPa) shows very low dislocation densities but similar reaction rates compared to spinel formation between single-crystal reactants at 29 MPa (Figs. 3–4). Regardless of the substrate, the observed dislocation density in spinel is generally increased at higher stresses. However, significant enhancement of the reaction layer thickness, of the effective diffusivities D_{eff} and related reaction rates are only observed, when the grain boundary character distribution changes with increasing stress. This occurs only for spinel formation between single crystals.

Enhancement of bulk diffusion due to migrating grain boundaries is largely excluded by the microstructure observations. Epitactic relations between spinel and sapphire remain intact during layer growth suggesting that grain boundary migration and recrystallization remain subordinate.

The change in grain boundary character distribution and the fragmentation of periclase-grown spinel into numerous subgrains is probably caused, at least to some degree, by dislocation creep accommodated subgrain rotation (Poirier 1985). During the experiment at 29 MPa, the samples shortened substantially, which in combination with results from TEM investigations supports the view that deformation occurred by dislocation creep.

At 29 MPa, further evidence for subgrain rotation is given by the microstructure of those grains, which grew epitaxial after sapphire (i.e., red grains in Fig. 2e). These grains rotate about the [111] axis, which is perpendicular to the reaction interface and parallel to the grain boundary traces. Thereby, the poles of {110} describe a great circle distribution perpendicular to [111] which, in combination with stereological considerations, suggest the formation of tilt subgrain boundaries associated with {110} glide planes. This suggests that deformation occurred at least in part by {110} slip (Fig. 2f). It is well known that deformation in spinel can occur by {110} slip, in particular this may happen in non-stoichiometric spinel (Mitchel et al. 1976). The deformation properties of spinel depend on its stoichiometry with substantial softening toward alumina-rich spinels (Corman 1992; Mitchel et al. 1976). Thus, differences in microstructure between sapphire and periclase-grown spinel are possibly caused by different rheological properties in combination with different epitaxial relations to the respective reactant.

However, external mechanical stress apparently influences epitactic growth and related nucleation and initial growth kinetics. Thus, it is entirely possible that the grain boundary character distribution is, in fact, already determined during the nucleation and initial growth and that deformation during later growing stages leads only to minor modifications. Our results suggest that nucleation or the formation of the first or the first few complete atomic layers of spinel can occur on either one or simultaneously on both of the reactants and that the spinel layers may grow layer by layer, where the smallest stable nucleus extends overwhelmingly in 2D or as islands, where the smallest stable clusters nucleate on the substrate then grow in three dimensions. We suggest a similar mechanism for the initial growth of the first atomic layers as it is described for layer growth during the deposition of thin films on single crystals. Thus, we use a terminology in analogy to surface sciences. At low stress, spinel grows epitactic after sapphire, which implies the formation of the first atomic layers of spinel on sapphire. For such a case, the first periclase-grown spinel layers likely nucleated on spinel formed from sapphire, which implies some retardation for periclase-grown spinel during nucleation. Epitactic nucleation of periclase-grown spinel on sapphire is also a possible scenario but unlikely due to the expected high activation barrier at lower stresses (see above). At intermediate stresses, there is the formation of two epitactic spinel layers, which formed from sapphire and periclase, respectively. This suggests simultaneous nucleation of spinel layers on periclase and sapphire, respectively. At even higher stresses, there is again the formation of two spinel layers. A first one grows epitactically after periclase and forms from periclase, whereas a second one forms from sapphire and consists of grains that grow epitactic after sapphire, grains that show a weak epitaxy after periclase, and grains lacking any epitactic relations. These relations again suggest simultaneous nucleation of spinel layers on periclase and sapphire, respectively, but with a significant change in growth mode for nucleation on sapphire, where growth apparently occurred in form of islands with different crystallographic orientations. It is speculated that these islands then extend or migrate in 2D forming an atomic layer that is composed of regions with different crystallographic orientions, which determine the microstructure of the later reaction rim.

Implications

Our results bear implications for process, where transport properties in polycrystals are important. Primarily, this work addresses polycrystalline reaction layer growth, a phenomenon that is known from many different materials and for a large range of physical conditions, including such diverse processes as oxidation of metals at atmospheric conditions and growth of new phases under extreme conditions in the Earth's interior. Moreover, solid-state reaction layer growth is a widely used method in engineering and designing materials with tailored properties. So far, neither the Earth nor material science communities have experimentally exploited the effects of non-hydrostatic stress on reaction layer growth: probably due to expected small scientific and/or technological returns. The fact that epitactic relations in spinel-forming reactions depend on stress is of prime importance in understanding chemical and structural changes at moving phase boundaries, and hence of indispensable value in designing new materials. Furthermore, there is a first-order dependence of solid-state reaction rates on non-hydrostatic stress. Thus, universally accepted growth models that may be appropriate at near atmospheric pressures or hydrostatic stress must be validated cautiously when applied to layer growth that occurs at different stress states. Non-hydrostatic stress is a well-known phenomenon in the Earth's crust and mantle and considerations of reactions rates and component mobilities need to consider the effects of stress on these properties.

Finally, we address implications of stress-induced grain boundary structure modification. Grain boundaries are ubiquitous and they influence the behavior of polycrystals. We show that ionic mobility in a polycrystal depends on its grain boundary character distribution and on the grain boundary structures, which depend on stress and deformation. Ionic mobility is directly related to both electrical conductivity and diffusivity and hence a wide range of bulk material properties is influenced by grain boundary structure modifications. We contend that modifications in grain boundary character distribution can be as important as grain size on bulk properties. For example, it has been suggested that conductivity contrasts of 1.5–2 orders in magnitude in the upper mantle might be caused by grain size reduction from 1 cm to 1 μm due to shearing (Ten Grotenhuis et al. 2004). However, Equation 6 of Ten Grotenhuis et al. (2004) shows that this holds only if the ratio D_{gb}/D_{vol} at the final deformation state exceeds 10^4. Because coincidence site lattice (CSL) grain boundaries (low Σ values) are boundaries of relatively low energy they should be abundant in a natural polycrystal and hence grain boundary diffusion should be slow, particularly in the undeformed state. If either D_{gb}/D_{vol} or σ_{gb}/σ_{vol} is low ($<10^3$) prior to deformation then bulk transport properties increase only 0.5 order of magnitude despite a decrease in grain size of 4 orders of magnitude. In such a case grain boundary structure modification during deformation becomes a viable process to increase the bulk conductivity by 1–2 orders of magnitude. This alternative explanation should be considered when interpreting magnetotelluric conductivity anomalies for the upper mantle, previously attributed to the presence of partial melt or volatiles (Roberts and Tyburczy 1999; Karato 1990).

Acknowledgments

This research was supported through the German Research Foundation (DFG) through grant AB 314/2-1, which pertains to FOR 741 DFG research group. A

constructive review by R. Joesten and B. Watson helped to improve the manuscript substantially. We thank Charles Lesher for valuable and constructive comments and suggestions. Willy Tschudin and Stefan Gehrmann are thanked for the careful preparation of the samples. R. Wirth is thanked for his help at the TEM.

REFERENCES CITED

Ashworth, J.R. and Sheplev, V.S. (1997) Diffusion modeling of metamorphic layered coronas with stability criterion and consideration of affinity. Geochimica et Cosmochimica Acta, 61, 3671–3689.

Balluffi, R.W., Brokmana, A., and King, A.H. (1982) CSL/DSC lattice model for general crystal-crystal boundaries and their line defects. Acta Metallurgica, 30, 1453–1470.

Carlson, W.D. and Johnson, C.D. (1991) Coronal reaction textures in garnet amphibolites of the Llano Uplift. American Mineralogist, 76, 756–772.

Carter, C.B. and Schmalzried, H. (1985) The growth of spinel into Al_2O_3. Philosophical Magazine A, 52, 207–224.

Corman, G.S. (1992) Creep of MgO-rich spinel single crystals. Journal of Material Sciences Letters, 11, 1657–1660.

Fisher, G.W. (1978) Rate laws in metamorphism. Geochimica et Cosmochmica Acta, 42, 1035–1050.

Fisler, D.K. and Mackwell, S.J. (1994) Kinetics of diffusion-controlled growth of fayalite. Physics and Chemistry of Minerals, 21, 156–165.

Freund, D., Wang, Z., Rybacki, E., and Dresen, G. (2004) High-temperature creep of synthetic calcite aggregates: Influence of Mn-content. Earth and Planetary Science Letters, 226, 433–448.

Götze, L.C., Abart, R., Rybacki, E., Keller, L.M., Petrishcheva, E., and Dresen, G. (2010) Reaction rim growth in the system MgO-Al_2O_3-SiO_2 under uniaxial stress. Mineralogy and Petrology, 99, 263–277, DOI:10.1007/s00710-009-0080-3.

Hallstedt, B. (1992) Thermodynamic assessment of the system MgO-Al_2O_3. Journal of the American Ceramic Society, 75, 1497–1507.

Harrison, L.G. (1961) Influence of dislocations on diffusion kinetics in solids with particular reference to alkali halides. Transactions of the Faraday Society, 57, 1191–1199.

Hay, R.S. (1994) Kinetics if deformation during the reaction of yttrium-aluminum perovskite and alumina to yttrium-alumina garnet. Journal of the American Ceramic Society, 77, 1473–1485.

Heidelbach, F., Terry, M.P., Bystricky, M., Holzapfel, C., and McCammon, C.A. (2009) A simultaneous deformation and diffusion experiment: Quantifying the role of deformation in enhancing metamorphic reactions. Earth and Planetary Science Letters, 278, 386–394. DOI:10.1016/j.epsl.2008.12.026.

Hesse, D., Senz, S.T., Scholz, R., Werner, P., and Heydenreich, J. (1994) Structure and morphology of the reaction fronts during the formation of $MgAl_2O_4$ thin films by solid state reaction between R-cut sapphire substrates and MgO films. Interface Science, 2, 221–231.

Humphreys, F.J. and Hatherly, M. (1995) Recrystallization and Related Annealing Phenomena, 619 p. Elsevier, Amsterdam.

Irving, B.A. (1964) Effect of grain boundaries on the diffusional growth of oxides on metals. Nature, 204, 1082–1083.

Joesten, R. (1991) Grain-boundary diffusion kinetics in silicate and oxides minerals. In J. Ganguly, Ed., Diffusion, Atomic Ordering, and Mass Transport, p. 345–395. Springer, Berlin.

Joesten, R. and Fisher, G.W. (1988) Kinetics of diffusion-controlled mineral growth in the Christmas Mountains (Texas) contact aureole. Geological Society of America Bulletin, 100, 714–732.

Kaur, I., Mishin, Y., and Gust, W. (1995) Fundamentals of grain boundary and interphase boundary diffusion, 3rd ed. Wiley, Chichester.

Karato, S. (1990) The role of hydrogen in the electrical conductivity in the upper mantle. Nature, 347, 272–273.

Keller, L.M., Abart, R., Wirth, R., Schmid, D., and Kunze, K. (2006) Enhanced mass transfer through short circuit diffusion: Growth of garnet reaction rims at eclogite facies conditions. American Mineralogist, 91, 1024–1038.

Keller, L.M., Wirth, R., Rhede, D., Kunze, K., and Abart, R. (2008) Asymetrically zoned reaction rims: assessment of grain boundary diffusivities and growth rates related to natural diffusion controlled mineral reactions. Journal of Metamorphic Geology, 26, 99–120.

Kenkmann, T. and Dresen, G. (1998) Stress gradients around porphyroclasts: Palaeopiezometric estimates and numerical modeling. Journal of Structural Geology, 20, 163–173.

King, A.H. and Shekhar, S. (2006) What does it mean to be special? The significance and application of the Brandon criterion. Journal of Material Sciences, 41, 7675–7682.

Koch, E. and Wagner, C. (1936) Über die Bildung von Ag_2HgJ_4 aus AgJ und HgJ_2 durch Reaktion im festen Zustand. Zeitschrift für Physikalische Chemie, 34, 317–321.

Mitchel, T.E., Hwang, L., and Heuer, A.H. (1976) Deformation in spinel. Journal of Material Sciences, 11, 264–272.

Poirier, J.-P. (1985) Creep of Crystals. High-temperature Deformation Processes in Metals, Ceramics and Minerals. Cambridge University Press, U.K.

Roberts, J.J. and Tyburczy, J.A. (1999) Partial-melt electrical conductivity: Influence of melt-composition. Journal of Geophysical Research, 104, 7055–7065.

Rossi, R.C. and Fulrath, R.M. (1962) Epitaxial growth of spinel by the reaction in solid state. Journal of the American Ceramic Society, 46, 145–149.

Saylor, D.M. and Rohrer, G.S. (2002) Determining crystal habits from observations of planar sections. American Ceramic Society, 85, 2799–2804.

Saylor, D.M., Morawiec, A., and Rohrer, G.S. (2003) Distribution of grain boundaries in magnesia as a function of five macroscopic parameters. Acta Materialia, 51, 3663–3674.

Schmalzried, H. (1962) Reaktionsmechanism der Spinellbildung im festen Zustand. Zeitschrift für Physikalische Chemie Neue Folge, 33, 111–128.

——— (1981) Solid State Reactions, 2nd ed., 254 p. Verlag Chemie, Weinheim.

Sheng, Y.J., Wasserburg, G.J. and Hutcheon, I.D. (1992) Self-diffusion of magnesium in spinel and in equilibrium melts: Constraints of flash heating of silicates. Geochimica et Cosmochimica Acta, 56, 2535–2546.

Stünitz, H. and Tullis, J. (2001) Weakening and strain localization produced by syn-deformational reaction of plagioclase. International Journal of Earth Science, 90, 136–148.

Sutton, A.P. and Baluffi, R.W. (1995) Interfaces in Crystalline Materials, 819 p. Clarendon Press, Oxford.

Ten Grotenhuis, S.M., Drury, M.R., Peach, C.J., and Spiers, C.J. (2004) Electrical properties of fine-grained olivine: Evidence for grain boundary transport. Journal of Geophysical Research, 109, B06203.

Watson, B.E. and Price, J.D. (2002) Kinetics of the reaction $MgO + Al_2O_3 = MgAl_2O_4$ and Al-Mg interdiffusion in spinel at 1200 to 2000 °C and 1.0 to 4.0 GPa. Geochimica et Cosmochimica Acta, 66, 2123–2138.

Wheeler, J. (1987) The significance of grain-scale stresses in the kinetics of metamorphism. Contributions to Mineralogy and Petrology, 97, 397–404.

Whitney, W.P. and Stubican, V.S. (1971) Interdiffusion studies in the system MgO-Al_2O_3. Journal of Physics and Chemistry of Solids, 32, 305–312.

Yund, R.A. (1997) Rates of grain boundary diffusion through enstatite and forsterite reaction rims. Contributions to Mineralogy and Petrology, 126, 224–236.

Zhang, P., Debroy, T., and Seetharman, S. (1996) Interdiffusion in the MgO-Al_2O_3 Spinel with or without some dopants. Metallurgical and Materials Transactions A, 27A, 2105–2114.

MANUSCRIPT RECEIVED AUGUST 15, 2009
MANUSCRIPT ACCEPTED JUNE 15, 2010
MANUSCRIPT HANDLED BY CHARLES LESHER